

Adventures in High-Temperature Resistive Emitter Physics

Steve Solomon

Acumen Consulting, P.O. Box 6084, Santa Barbara, CA 93160

Paul Bryant

Santa Barbara Infrared, Inc., 30 S. Calle Cesar Chavez, Suite D, Santa Barbara, CA
93103

ABSTRACT

The next generation of resistively heated emitter pixels is expected to attain apparent temperatures more than a factor of two higher than presently achievable – in excess of 2000 K. The peak temperatures for the current generation of devices are determined by the balance between the power input to the pixel and the conductive loss of heat through the leg structures. At pixel temperatures higher than approximately 1500-2000 K, radiative losses will begin to dominate over conductive losses. We explore the physics of this regime and find that the peak temperature is determined primarily by the power input, emissivity and emitting area. The speed of radiatively limited pixels is also examined and found to be considerably more complicated than that of conductively limited pixels since both loss terms play significant roles in the pixel's dynamic behavior. In order to attain the higher temperatures required, development work will be required on two fronts: materials science and advanced, higher power drive circuitry. Some of the critical issues related to these tasks are discussed.

Keywords: Resistive emitter, material science, radiatively limited pixels, device physics, thin films.

1. Introduction

To date, every generation of resistively heated IR scene projectors has been limited by conductive losses; pixel-level radiative losses have played a relatively small role even though these losses are its *raison d'être*. As apparent temperatures rise with successive generations of emitter devices, the physical temperatures attained by the pixels rises still faster. The power loss in the pixel will, at some temperature, become dominated by the radiative term, making the pixel more efficient in terms of converting input power to radiant power. This transition temperature will be determined by the thermo-physical properties of the pixel's constituent materials, geometry and the power input.

Resistive heating technology is the most mature of the myriad IR scene projection technologies available today; it has the longest developmental history, the largest number of units in the field, and the best overall performance figures of merit in terms of speed, dynamic range, temperature resolution, flickerless emission, broadband output, greater than 512^2 spatial resolution, and high frame rates. These factors make resistive emitters the most appropriate and realistic foundation on which to base the development of the next generation of high dynamic range IR scene projectors. Unfortunately, the materials used in fabricating existing generation of devices are not stable at the extreme temperatures required for the next generation of devices (~3000 K or higher) – the pixel will melt well before attaining the required temperatures.

Attaining the temperatures required for future MDA weapons system simulations such as targets with hot engine exhausts, rocket plumes and infrared countermeasures will require development on numerous fronts, the most challenging and difficult of which is the selection of the materials of which the emitter pixels are fabricated. These new materials must 1) be stable (*i.e.* repeatable) over the temperature range 300 K – 3000 K, 2) possess thermo-physical properties suitable for the operating temperature and speed requirements and 3) be compatible with thin-film processing requirements. These 3 broad requirements will be further discussed in the context of high temperature resistively heated IR scene projector pixels.

2. Pixel Physics

We will, in the ensuing analyses, consider the steady state as well as the dynamic behavior of an emitter pixel when radiative losses play a significant role in determining temperature and speed. For the purposes of the analyses presented here, we assume that the conductance and thermal mass of the pixel are independent of temperature. Unless otherwise specified, the pixel geometry used in calculating the numerical predictions is that of the LFRA array¹:

Parameter	Value
Pixel pitch	48 μm
Leg Length	25 μm
Emissivity	0.8
Fill factor	50%
Pixel type	Gossamer (50% thin)

Table 1 – Pixel parameters used in numerical simulations, which are identical to the LFRA emitter array design values.¹

Before delving into the device physics, we calculate the pixel temperature as a function of MWIR (3-5 μm) apparent temperature for the pixel parameters listed in Table 1. The results of this calculation are shown in Figure 1, from which we see that attaining apparent temperatures on the order of 2000 K will require pixel temperatures of ~ 3000 K. This is comparable to the surface temperatures of late type M stars such as Betelgeuse or Antares. These temperatures will play a large role in determining the suitability of any material set selected for fabricating high temperature devices; material requirements are discussed in more detail in section 3.

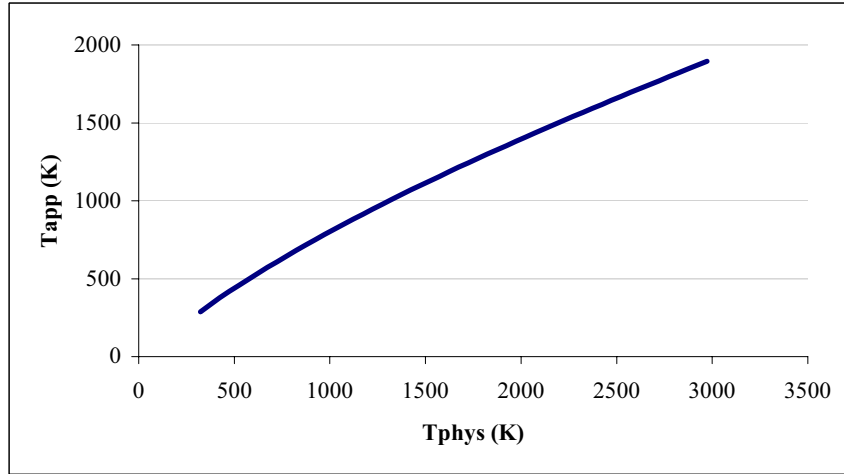


Figure 1 – Apparent MWIR temperature vs. pixel temperature for the pixel parameters shown in Table 1 for unity optical throughput.

The pixel's behavior is governed by the first order differential equation:

$$c \frac{dT}{dt} = P_{in} - G(T - T_s) - \sigma A \sum_i f_i \varepsilon_i (T^4 - T_i^4) \quad (1)$$

where c is the pixel's thermal mass, T is the pixel temperature, T_s is the substrate temperature, P_{in} is the input power, G is the total conductance of the legs, σ is the Stefan-Boltzmann constant, A is the pixel's emitting area, f_i is a geometrical (view) factor associated with each of the different temperatures (T_i) into which the pixel is radiating and ε_i is the emissivity factor, which includes the emissivities of the

emitting pixel as well as that for each of the backgrounds into which the pixel is radiating. In order to simplify the analysis, we collapse the radiative loss terms into a single “effective” term as follows:

$$\sum_i f_i \varepsilon_i (T^4 - T_i^4) \approx \beta (T^4 - T_{bg}^4) \quad (2)$$

where we have combined the geometrical and emissive terms into the constant β , and defined an effective background temperature (T_{bg}) into which the pixel is radiating. Though this effective background temperature will be on the order of 300 K, its precise value is almost inconsequential in determining the steady state temperature due to the fourth power dependence. The constant β is expected to be approximately 0.5 based on geometrical considerations.² Equation (1) then becomes:

$$c \frac{dT}{dt} = P_{in} - G(T - T_s) - \sigma A \beta (T^4 - T_{bg}^4) \quad (3)$$

2.1. Radiative Limit

Steady state - It is instructive to consider the limiting case where the pixel’s conductive losses vanish. Setting the conductive term in equation (3) to zero, and solving for the steady state temperature as $t \rightarrow \infty$, we find

$$T = \left[\frac{P_{in}}{\sigma A \beta} + T_{bg}^4 \right]^{1/4} \approx \left[\frac{P_{in}}{\sigma A \beta} \right]^{1/4} \quad (4)$$

Note that since we have neglected the conductive term, the leg length plays no role in determining the final temperature attained by the pixel. In the radiatively limited regime, the steady state temperature will be dictated primarily by the power input, the emitting area and emissivity, and is seen to be a weak function of these three parameters. In comparison, the pixel temperature for the conductively limited case exhibits a linear dependence on power. Figure 2 shows the pixel temperature predicted by equation (4) as a function of both pixel input power and the parameter β . This plot indicates the importance of minimizing the emissive surfaces that the pixel “sees” in order to minimize β to attain the highest possible temperatures at the lowest possible power inputs.

For a radiatively limited pixel, reducing the emitting area will increase the physical temperature because it reduces the radiative losses. In contrast, a conductively limited pixel’s temperature is independent of fill factor. In terms of apparent temperature, the radiative and conductive pixels exhibit comparable dependence on fill factor. In this case, it may prove advantageous to design as large an emitting area as is reasonable in order to 1) keep the pixel temperature as low as possible so as not to unnecessarily stress the materials, 2) increase apparent temperature, and 3) lower the temperature at which radiative losses dominate the pixel’s power balance, which will minimize the required drive capacity of the CMOS (see discussion in next section). In both cases, increasing the pixel’s emitting area (and hence its thermal mass) will degrade speed, but the dependence of speed on thermal mass is weaker for the radiatively limited pixel than it is for the conductively limited case.

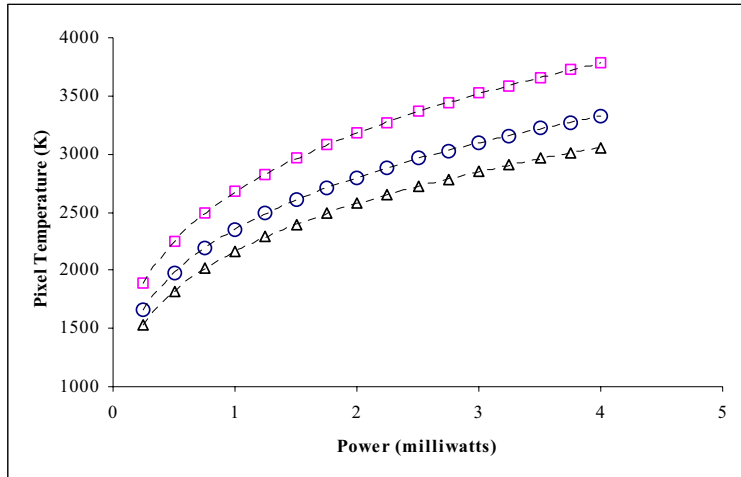


Figure 2 – Pixel temperature vs. input power for three different values of β , the combined emissive and geometrical factor.

Dynamic Behavior - The temporal evolution of the radiatively limited pixel is instructive in that it provides insights into the physical mechanisms associated with how purely radiative losses affect pixel speed. Figure 3 illustrates the temporal behavior of a radiatively limited pixel. The 10-90% radiative rise time is 2.3 ms while the 100-10% radiative fall time is 15.3 ms. The rise time is very rapid because there are no conductive losses as the pixel starts heating, which results in the maximum possible heating rate allowed by the input power and material properties. As the radiative losses begin to evidence themselves at high temperatures (above ~ 2000 K), the pixel finally begins to slow down after its initial rapid rise. In previous generations of emitters, the fall time has been faster than the rise time owing to the radiative and conductive losses when the pixel is at high temperatures, with conductive losses dominating at lower temperatures. In the instance under consideration here (zilch conductive losses), we see that the pixel has a very difficult time cooling radiatively to temperatures below ~ 1000 K, hence the very long fall time.

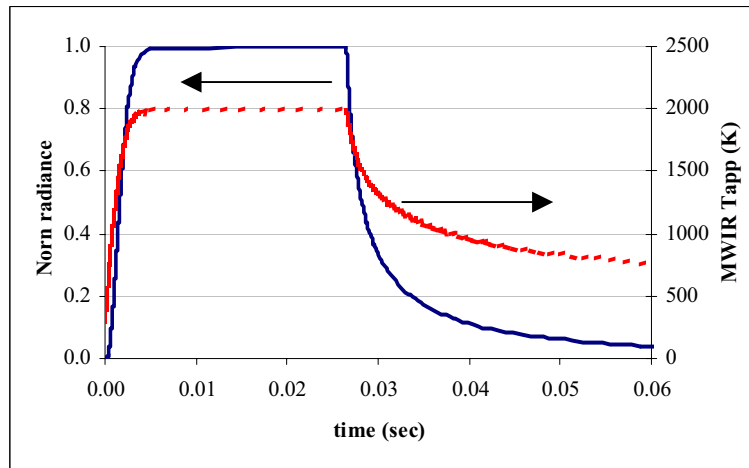


Figure 3 – Temporal behavior of radiatively limited pixel with the parameters found in Table 1 and a drive power of 3 mW. Note the order of magnitude difference between the rise and fall times.

The radiatively limited rise time will be determined by the power input to the pixel (more power means a faster pixel) and by the emitting area and emissivity (more of each mean lower temperature). Note that power does not help fall time in the sense that the pixel's cooling rate (dT/dt) is determined strictly by the losses once the power is turned off (see equation (1)).

2.2. Realistic Behavior

While the preceding discussion and analysis are helpful in gaining an understanding of the physical mechanisms at play in a radiatively limited pixel, it is not strictly indicative of how real-world pixels will perform, since any pixel fabricated in a terrestrial laboratory out of materials from the known periodic table of elements will include the effects of both radiative and conductive losses. While leg conduction does not contribute significantly to the maximum attainable temperature in the radiatively limited case, it will play a role in the speed of a pixel that starts heating at temperatures where the losses are dominated by thermal conduction. In this section, we consider how the two loss mechanisms play together to determine pixel performance, and we estimate the temperature that separates the two limiting cases, radiative and conductive.

Transition temperature - Equating the two loss terms enables us to determine the temperature at which radiative losses begin to dominate over conductive losses. We denote this transition temperature by T_{rad} .

$$G(T - T_s) = \sigma A \beta (T^4 - T_{bg}^4)$$

$$\rightarrow T_{rad} \approx \left[\frac{G}{\sigma A \beta} \right]^{1/3} \quad (5)$$

where we have used the approximations $T \gg T_s$ and $T^4 \gg T_{bg}^4$, which are valid at the high temperatures under consideration. Figure 4 illustrates the radiative temperature as a function of leg length for three different sets of material properties. In general, the radiative temperature values are seen to be very high, making it more difficult to attain pixels that are radiatively limited when the leg lengths are relatively short. Increasing the emitting area lowers the transition temperature; in other words, it lowers the temperature at which radiative losses start to dominate. This is important because it will lower the drive power required of the CMOS.

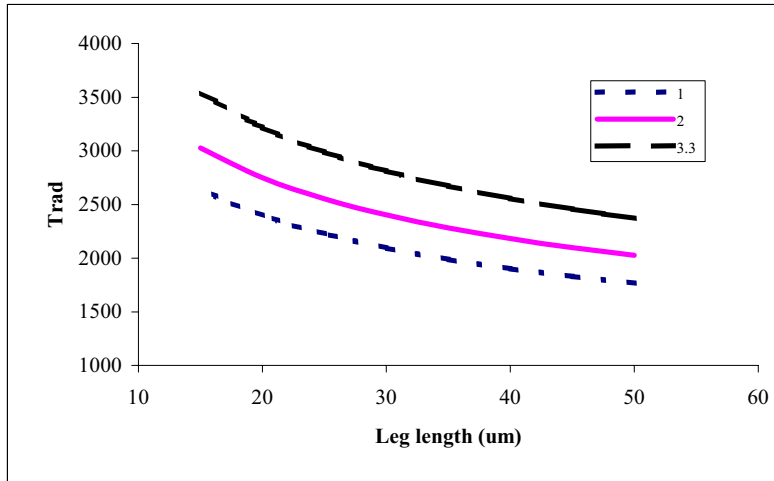


Figure 4 – Radiative temperature as a function of leg length for three different values of material thermal conductivity for a pixel power of 3 mW.

Steady State - Making use of the same approximations found in equation (5) in order to solve equation (3) for the steady-state temperature, we find that the steady state temperature is given by the solution to a quartic equation. The solution can be written in closed form, but is algebraically unpleasant and so will not be shown here.

$$\begin{aligned}
0 &= P_{in} - G(T - T_s) - \sigma A \beta (T^4 - T_{bg}^4) \\
&\approx P_{in} - GT - \sigma A \beta T^4 = P_{in} - G \left[T + \frac{T^4}{T_{rad}^3} \right]
\end{aligned} \tag{6}$$

The exact form of equation (6) was solved numerically and the results are plotted in Figure 5 as a function of input power for three different cases of conductance: zilch (radiatively limited), 25 and 50 μm legs. T_{rad} is also indicated on the curves, and as discussed previously, is seen to be higher for shorter legs.

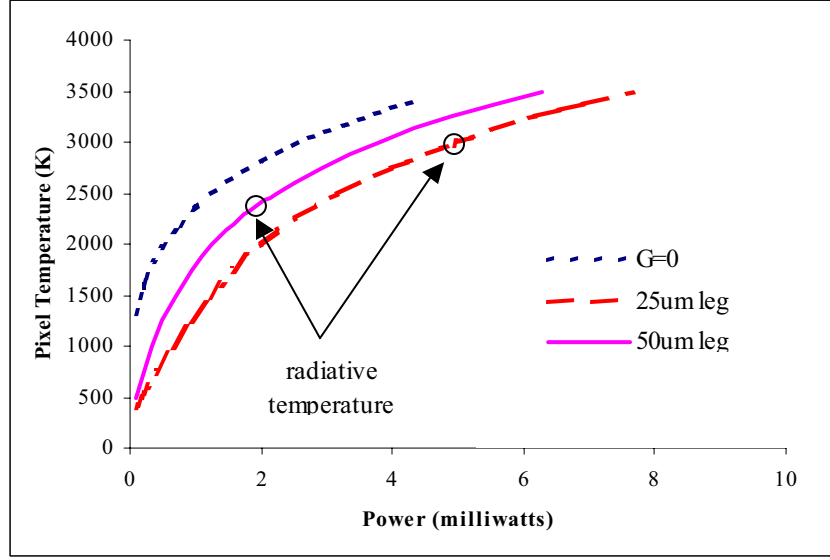


Figure 5 – Pixel temperature vs. power for three different pixel conductances: 0 (radiatively limited), 25 μm legs and 50 μm legs.

Dynamic Behavior - The dynamic behavior of a high temperature pixel is complicated by the fact that it will be dominated by both conductive as well as radiative losses at different times during its temporal evolution, and hence, both loss mechanisms will contribute to the speed of the pixel. No simple closed form solution for the pixel's time constant exists, so numerical solutions will be relied upon to guide the pixel design.

We calculate the time required to attain the radiative temperature (T_{rad}) in order to gain insight into the various dependencies that underlie the pixel's temporal behavior.

$$t(0 \rightarrow T_{rad}) \equiv t_{rad} \approx \frac{C}{P \left[\frac{\sigma A \beta}{G} \right]^{1/3} - 2G} \tag{7}$$

where we have assumed that $T_{rad} \gg T_{substrate}$. The first and second terms in the denominator represent the radiative and conductive contributions, respectively, to the radiative temperature. From equation (7), we see that t_{rad} is linear in the pixel's heat capacity in exactly the same fashion as the conductive pixel. As expected, the time to reach T_{rad} increases as the conductance increases, but in a more complicated fashion than in the conductively limited case.

At reduced power input levels, the speed of all resistively heated projector arrays is degraded and the

high temperature pixels under discussion are no exception to this rule. For the pixel geometry discussed above (see Table 1), the 10-90% risetime is ~10 ms and 15 ms for $T_{app}=1000$ K and 500 K, respectively. If faster temporal response is required at lower apparent temperatures, then the pixel can be further thinned or the output of a high temperature array could be optically combined with that of a lower temperature array.

Emissivity – The emissivity of the optical cavity (formed by the pixel and the underlying CMOS substrate) and the Planck function are both wavelength dependent, so a more appropriate emissivity term for use in calculating radiance and apparent temperature is the Planck averaged emissivity, which is defined as:

$$\mathcal{E}_{Planck} \equiv \frac{\int_{\lambda_1}^{\lambda_2} \varepsilon(\lambda)B(\lambda)}{\int_{\lambda_1}^{\lambda_2} B(\lambda)} \quad (8)$$

At the extreme temperatures under discussion, using a constant emissivity term can lead to errors on the order of 5% in radiance calculations. Using a polynomial fit to the numerically modeled emissivity for a typical stack geometry in (8), we find that the Planck emissivity is on the order of 5% lower than that of the average emissivity in the MWIR (3-5 μ m) at 3000 K pixel temperatures and ~5% higher than that of the average emissivity at 300 K pixel temperatures. In the LWIR band (8-12 μ m), \mathcal{E}_{Planck} is ~5% higher than the average emissivity at 3000 K and that there is virtually no difference at 300 K. Since apparent temperature is weakly dependent on the emissivity, the 5% differences calculated will only result in T_{app} differences on the order of 1%.

3. Material & Fabrication Issues

As a guide to selecting the desired material set for high temperature emitter pixels, we now review and discuss the properties desired for an ideal set of emitter pixel materials. All the materials should exhibit stable and repeatable thermo-physical properties over the temperature range 300-3000 K, be chemically inert and easy to deposit and etch. An ideal dielectric would have minimal specific heat (so that it responds rapidly) and minimal stress (so it does not deform appreciably) while maintaining exceptionally high mechanical strength (so it can support the pixel body over the temperature range), minimal CTE (so it does not bend too much with temperature and degrade the integrity of the optical cavity, or worse, result in plastic deformation) and be a perfect diffusion barrier (so that the metals cannot diffuse into them sufficiently to change its properties). The leg metal should have minimal thermal conductivity (so that the conductance is dominated by the dielectric), and high electrical conductivity (so that it does not take power away from the pixel). The absorber material should exhibit minimal TCR (thermal coefficient of resistance) and be free of absorption features over the intended spectral range of the emitter. Finally, the resistor material should be stable with respect to TCR over its intended operating range, have repeatable annealing properties and be transparent in the infrared.

At the extreme temperatures required, it is important that the conductive losses be negligible in comparison to the radiative losses so that the devices are more efficient, *i.e.* so that the power delivered to the pixel is converted to radiation as efficiently as possible. This will limit the power required from the CMOS drive circuitry. This requirement places stringent limits on the conductive losses of the pixel, and hence, the thermal conductivity of the dielectric both in terms of magnitude as well as its temperature dependence. In general, thermally isolating, electrically conductive legs are desired.

3.1. Material stability

Materials typically cease to behave in a linear and elastic fashion at extreme temperatures. A high melting point will, in general, result in a more stable material at elevated temperatures. Behaviors such as creep and relaxation are thermally activated, and there are a wide variety of physical phenomena that result in changes to material properties, some of which are structural (*e.g.* phase changes & recrystallization,

grain growth, densification/stress) and some of which are compositional/stoichiometric changes (e.g. diffusively or thermally driven chemical changes such as oxidation).

Material stability over the intended temperature operating range of the devices is a crucial prerequisite for the material set, but the annealing process also places requirements on the material properties at temperatures higher than those of the nominal operating conditions. Ideally, the material set will be non-reactive and effective diffusion barriers will keep compositional film changes to a minimum so that any annealing changes are small and relatively easy to understand. These ideal conditions will be difficult to realize. Thermodynamic considerations of ideal material interfaces should be employed in the selection of the materials in order to increase the probability of success by calculating the degree of interfacial stability as given by the possible reaction enthalpies.

3.2. Thermo-physical properties

There is very little reliable information available regarding thermo-physical properties for the thin film formats required of resistive emitter technology at elevated temperatures. Most of the available high temperature data falls in the range 1000-1500 K, and is predominantly for bulk materials rather than thin films. Thin films properties are typically very different from their bulk counterparts due to the method and details of deposition, and the fact that interfaces between films often plays a major role in the film properties, which means that thin films with the same nominal stoichiometry can possess very different thermo-physical properties. We will now briefly discuss the relevant material properties.

Specific heat – this material property, in tandem with the pixel’s mass, determines the speed of the pixel. The specific heat of the bridge structure should, in general, be kept as small as possible consistent with the mechanical strength required to maintain the pixel’s integrity. Specific heat is very difficult to measure at the pixel level because the mass is in the nanogram range; the best microcalorimeters are only capable of measuring samples in the microgram range.

Thermal conductivity – this material property determines the conductance of the pixel legs, which trades speed for temperature for a given power input. The thermal diffusivity, in conjunction with the specific heat, determines the thermal conductivity of the material, so this property may be substituted, but is generally more difficult to measure. All measurements of thermal conductivity on thin films are complicated by surface conductivity contributions – thinner films have a proportionally larger surface contribution.

Electrical resistivity/conductance – this property, in conjunction with the CMOS drive capability, dictates the electrical power available for heating the pixel. Therefore, the electrical resistivity of the pixel drives both speed and temperature performance parameters. While this is not particularly difficult to measure, it is important that the TCR be small enough so that the CMOS is able to provide the required drive over the resistance (load) range expected. In addition, the TCR must exhibit the proper sign for the CMOS drive mode so as not to result in thermal runaway.

Optical properties – the index of refraction and absorption coefficient play roles in the thickness of the dielectric and absorber, respectively. The temperature behavior and stability will have to be determined to optimize device performance for whatever materials are selected.

Given this poor knowledge base and the manifold sources of variability, an important portion of the work required to attain higher temperature emitter materials will involve developing the capability to measure the important material properties over a wide temperature range. There are a variety of techniques in the literature for measuring these properties; much of the difficulty lies in the extreme temperatures at which these properties have to be determined. Among the methods are: the three omega (3ω) method³, laser flash⁴, photopyroelectric⁵, and the amplitude method.⁶

3.3. Thin Film Processing

The materials out of which emitter pixels are fabricated must be compatible with thin film processing. Even if the new materials are thin-film capable, care must be paid to method by which the films are deposited: it is preferable that the films be capable of deposition at low temperatures so that the emitter structures can be fabricated directly on the CMOS. The use of a low homologous temperature enormously restrains atomic surface mobility, resulting in porous columnar structure due to self-shadowing. This type of material microstructure may be beneficial for the bridge structure in that it will have low specific heat, but the thermal conductivity and mechanical strength of such structures is likely to be low. Both experiment and kinetic Monte Carlo simulations indicate that increasing the substrate temperature during deposition can be very effective in transforming more porous thin films to the dense structures required for high temperature pixels. Unfortunately, high processing temperatures will destroy the CMOS, which would then require yet another development task: that of fabricating the emitters independently from the CMOS and mating them together at the end of the process. This work has been successfully developed elsewhere^{7,8}, but transferring this technology to the emitter fab will require considerable time and expense.

The deposition method and the specific deposition parameters employed for the fabrication of the films is crucial to the film's properties. Physical vapor deposition (*e.g.* sputtering) and chemical vapor deposition (*e.g.* plasma) are the two most common techniques, but other techniques (*e.g.* atomic layer deposition) will also be considered. Discussions with thin film foundries and literature review will be employed in the selection of potential deposition methods.

4. Summary

The physics of extremely high temperature resistively heated emitter arrays has been developed. We have found that in order to attain MWIR apparent temperatures in the 2000 K range, pixel temperatures on the order of 3000 K will be required. Radiative power losses from the pixel were found to play a large role in the device performance, and result in different relationships between input power, emissivity and emitting area and pixel temperature. In addition, radiative losses rather than power input dictate the maximum pixel temperature to first order. The temporal behavior of radiatively limited pixels was found to be distinct from that of conductively limited pixels: the fall time of radiatively limited pixels can be considerably longer than the rise time. Attaining the required temperatures will also necessitate approximately a five-fold increase in the power delivered to the pixel compared with the present generation of CMOS devices (*e.g.* LFRA). In addition, new materials will be required in order to support the high temperatures required, which necessitates a materials development task in order to realize operational high temperature devices.

Acknowledgements

The authors would like to thank Barry Cole and the Honeywell gang for lighting the way. Owen Williams at DSTO has been a very valuable source of experience and insight and Don Snyder at Eglin AFB has provided many thought-provoking discussions.

REFERENCES

- ¹ P. Bryant, J. Oleson, B. Lindberg, K. Sparkman, S. McHugh and S. Solomon, *SPIE Proc. HWIL Testing VIII*, **5092**, this volume, 2002.
- ² F. Incropera, D. DeWitt, *Fundamentals of Heat and Mass Transfer* (5th Ed.), Wiley & Sons, New York
- ³ D. Cahill, *Rev.Sci.Instrum.*, **62**,802, 1990.
- ⁴ M. Krishnaiah, G. Seenivasan, P.S. Murti, *Rev.Sci.Instrum.*, **73**, 3353, 2002.
- ⁵ M. Marinelli, U. Zarmmit, F. Mercuri, R. Pizzoferrato, *J.Appl.Phys.*, **72**, 1096, 1992.
- ⁶ X. Zhang, C.P. Grigoropoulos, *Rev.Sci.Instrum.*, **66**, 1115, 1995.
- ⁷ F. Niklaus, E. Kalveston, G. Stemme, *SPIE Proc. IR Technology & Applic. XXVII*, **4369**, 397, 2001.
- ⁸ S. McHugh, J. Warner, M. Pollack, A. Irwin, T. Hoelter, B. Parrish, and J. Woolaway, *SPIE Proc. HWIL Testing IV*, **3697**, 209, 1999.